High vacuum metallurgy – opportunities in lunar resource processing

Conference Paper · December 2021

5 authors, including:

Matthew Shaw
The Commonwealth Scientific and Industrial Research Organisation
18 PUBLICATIONS **94** CITATIONS

SEE PROFILE

Geoffrey Brooks
Swinburne University of Technology
311 PUBLICATIONS **4,811** CITATIONS

SEE PROFILE

M Akbar Rhamdhani
Swinburne University of Technology
297 PUBLICATIONS **3,869** CITATIONS

SEE PROFILE

Mark I. Pownceby
The Commonwealth Scientific and Industrial Research Organisation
258 PUBLICATIONS **4,836** CITATIONS

SEE PROFILE

High vacuum metallurgy – opportunities in lunar resource processing

M G Shaw[1], G A Brooks[2], M A Rhamdhani[3], A R Duffy[4] and M I Pownceby[5]

1. PhD Candidate, Swinburne University of Technology, Melbourne Vic 3122.
   Email: mgshaw@swin.edu.au
2. Professor, Swinburne University of Technology, Melbourne Vic 3122.
   Email: gbrooks@swin.edu.au
3. Professor, Swinburne University of Technology, Melbourne Vic 3122.
   Email: arhamdhani@swin.edu.au
4. Professor, Swinburne University of Technology, Melbourne Vic 3122.
   Email: aduffy@swin.edu.au
5. Senior Principal Research Scientist, CSIRO Mineral Resources, Melbourne Vic 3168.
   Email: mark.pownceby@csiro.au

ABSTRACT

The effect of low-pressure environments on metal compound stability is a well-known but rarely utilised phenomenon, even though reduction processes operating at subatmospheric pressures offer significant benefits in terms of the energy requirements for metal compound reduction. At industrial scales, some vacuum metallurgical processes such as silicothermic reduction to produce magnesium metal via the Pidgeon process, routinely operate under low vacuum conditions ($\sim 10^{-5}$ atm). However, more often in terrestrial industry, the benefits of these vacuum conditions are counteracted by equipment availability, production rates, and higher operational costs. The use of high vacuum conditions ($< 10^{-10}$ atm) to promote the production of metals at significantly lower temperatures is rendered unviable by the lack of industrial scale vacuum pumping apparatus capable of attaining these pressures. The difficulty in obtaining ultra-low pressures at industrial scales combined with the seeming lack of need to focus on the reduction of energy requirements for metal compound reduction, results in vacuum metallurgical processes being overlooked for terrestrial applications. In contrast however, the challenge presented by the likely need for metal production in space for supplying future off-Earth activities has the opposite requirements. In space, and specifically on the Moon, access to electrical energy is significantly limited and extremely costly, and instead of high vacuum conditions requiring specialised pumping equipment, these conditions represent the natural ambient conditions found on the lunar surface. We predict that the development of low-pressure metal production technologies for use in space will heavily favour the field of vacuum metallurgy. In the current work we present a set of calculated Ellingham diagrams that demonstrate the effects of vacuum conditions on oxide stability at elevated temperatures and highlight the significant advantages these vacuum conditions can provide in the field of astrometallurgy.

INTRODUCTION

The use of vacuum conditions in processing operations has been a topic of study for many decades. However, despite the initial enthusiasm for the potential presented by vacuum metallurgy, very few current industrial processes use such conditions. The current interest in extra-terrestrial resource processing is driving a renewed interest in such implementations. Access to space, and the natural vacuum conditions found there, inherently lead to a much simpler implementation of vacuum metallurgy processes in this environment.

The current work will briefly review vacuum metallurgy, relevant history and uses, as well as explore some of the significant limitations that have led to its lack of application in modern industry. We will cover Ellingham diagram theory as a foundation to then present a novel set of Ellingham diagrams generated at vacuum conditions. The effect of such vacuum conditions on the stability of oxides and subsequent energy requirements for reduction will be explored. Finally, we comment on some of the limitations of high-vacuum metallurgy, on how the access to the vacuum of space will help promote research addressing these issues, and how terrestrial vacuum metallurgical applications will benefit from research in this area.

VACUUM METALLURGY

The beneficial effects of low pressure environments on some metallurgical processes is well documented (Browne, 1971; Kroll, 1951). Vacuum can be used as a replacement for an inert atmosphere; to promote the separation of product material via fractional distillation; to facilitate the degassing of molten metals to improve physical characteristics, and; to reduce the temperature requirement of reactions with gaseous products (Browne, 1971). Despite these benefits, very few large-scale processing operations utilise vacuum metallurgy. One of the few processes used industrially is the Pidgeon process, the silicothermic reduction of magnesium under vacuum.

The Pidgeon process, developed in the 1940s (Pidgeon and Alexander, 1944), saw a large rise in application especially within China since the first industrial application in 1978 (Zang and Ding, 2016). The silicothermic reduction of magnesium is undertaken at 1200 to 1500°C at pressures of 10^{-4} to 10^{-5} atm (Halmann, Frei and Steinfeld, 2008). Magnesium metal produced during this reduction is in a gaseous form which is then condensed to form a high purity (~99.97 per cent) magnesium 'crown'. This magnesium crown is then re-melted under inert atmosphere into ingots (Halmann, Frei and Steinfeld, 2008).

The silicothermic reduction of magnesium, is not thermodynamically favoured at 1 atm pressure and instead would require temperature conditions in excess of 2000°C. However, under vacuum conditions, reaction temperatures as low as 1000°C have been achieved (Wada *et al*, 2017). The use of low pressure in this manner, to reduce the thermal requirements of metallurgical reactors has also been explored for many other applications. For example, the carbothermic reduction of Al_2O_3, BeO, MgO, SiO_2, Fe_2O_3, TiO_2, ZrO_2, HfO_2, and GeO_2 are all favoured under vacuum conditions. The use of vacuum in these reactions lowers the required reaction temperature and has the added benefit of minimising complications due to carbide and oxycarbide formation (Halmann, Frei and Steinfeld, 2011).

Despite these demonstrated benefits of vacuum metallurgy, on Earth, the reduction in the thermal energy requirements of a process due to a vacuum environment is insufficient to counteract the increase in energy (ie cost) required by pumping apparatus' to maintain that low pressure environment (Balomenos, Panias and Paspaliaris, 2012). This means that unless there are other factors involved, for example highly reactive product materials which require a lack of air, the reduction of reactor temperatures in metallurgical operations due to vacuum conditions will not be viable as it results in a net increase in energy use. This is further amplified if pressures even lower than typical 'industrial vacuum' conditions were to be considered.

The term industrial vacuum is often used to refer to the pressure reached by traditional industrial sized rotary vacuum pumps, typically in the realm of between 1 to 10^{-5} atm (Roth, 1990; O'Hanlon, 2005). However pumping systems such as turbomolecular vacuum pumps can reach pressures of 10^{-10} atm (O'Hanlon, 2005). This raises the question as to what sorts of thermal energy savings could be made at such pressures. While industrial operation at these pressures would similarly result in a net increase in energy cost, turbomolecular pumping systems being significantly less efficient than rotary vacuum pumps (O'Hanlon, 2005), the potential thermal energy savings are at least intellectually intriguing.

Beyond the energy inefficiency of operating metallurgical reactors at high vacuum conditions, there are also other factors that make this sort of operation unlikely. The cost of such systems, the scalability, maintenance requirements, considerably lower pumping rates, and requirement for much more efficient sealing technology on any reactor, make the implementation of these systems doubtful in the near future with current pumping technologies. However, in the interest of better understanding the potential benefits of high-vacuum metallurgy, we will examine the thermodynamic effects of these low-pressure conditions in the current work with the use of Ellingham diagrams. This work however, is aimed at a future where high vacuum pumping systems are made more efficient and applicable to industrial application. Or, when free access to high and even ultra-high vacuum environments is made considerably easier, such as in the field of astrometallurgy, when operating reduction processes in space or on other celestial bodies.

ELLINGHAM DIAGRAMS

A common tool for the extractive metallurgist when examining the thermodynamic viability of any given proposed process involving chemical reactions is the Ellingham diagram. An Ellingham diagram is a graph showing the temperature dependence of the stability of compounds. This analysis is usually used to evaluate the ease of reduction of metal oxides and sulfides. In the current work we will briefly review some theory around Ellingham diagrams and then we will discuss the implications of pressure on oxide reduction mechanisms with reference to Ellingham diagrams generated at alternate total pressure conditions.

Ellingham diagram theory

The specific principles involved with most thermodynamic calculations when it comes to determining equilibrium states are the free energy functions, Gibbs free energy and Helmholtz free energy. These two functions calculate the free energy within a system at isothermal and isobaric conditions (Gibbs) and isothermal and isochoric conditions (Helmholtz) (Rosenqvist, 2004). In most thermodynamic calculations a constant pressure is assumed for all systems, and as such, Gibbs free energy is used most often. The function for Gibbs free energy can be seen in Equation 1 where G is the Gibbs free energy (J), H is enthalpy (J), T is temperature (K), and S is entropy (J/K).

$$G = H - TS \tag{1}$$

In an isothermal system, the ΔG of a reaction A→B is equal to G_B – G_A. There is no absolute value for G in this case however the ΔG can also be calculated as per Equation 2.

$$\Delta G = \Delta H - T \Delta S \tag{2}$$

In an isobaric and isothermal system, and in the absence of work beyond volume work, ΔG is negative for spontaneous reactions and zero for fully reversible processes. A reaction with a positive ΔG value will not proceed forwards in an isolated system (Rosenqvist, 2004). It is important to note that the ΔG of a reaction is not directly related to the kinetics of that reaction, a spontaneous reaction, especially at lower temperatures, may take a long time to occur (Rankin, 2011).

First constructed by Harold Ellingham in 1944 (Ellingham, 1944), the Ellingham Diagram is a visual representation of the changes in ΔG for the formation of a compound with respect to temperature. The most common Ellingham diagram is for oxide formation which is shown in Figure 1. The diagram is predicated on the idea that Equation 2 can be represented as a linear equation with ΔH being the intercept and -ΔS being the slope. After plotting a number of oxide reactions, Ellingham (1944) found that whilst changes in ΔH and ΔS do occur with temperature, the changes are small enough that they can be considered constants for the purpose of graphing. A change in ΔS will occur at phase transition points which are also marked on the diagram.
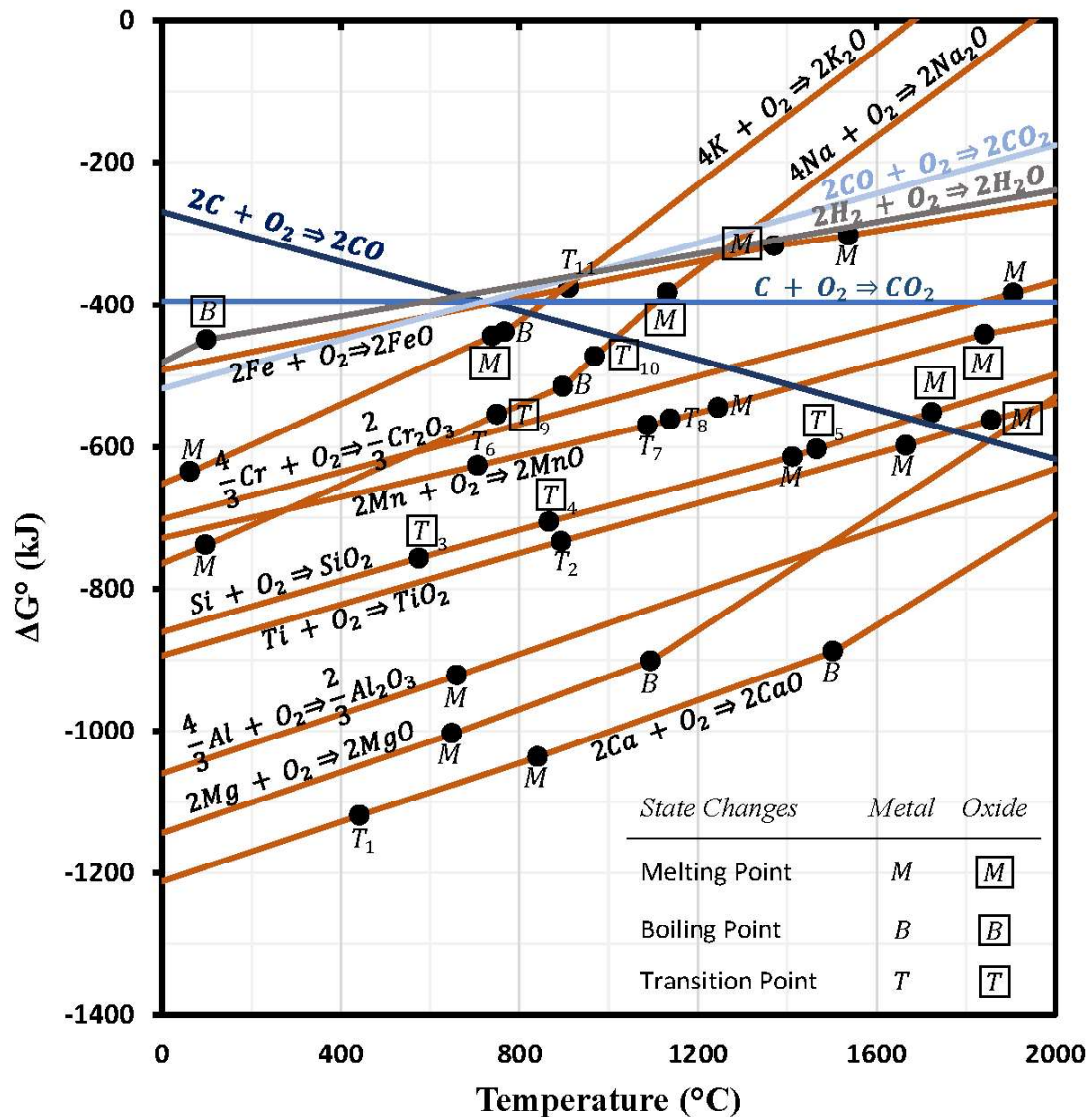
When considering the reduction of a metal oxide by another metal, any metal that is found lower on the diagram at the desired temperature can act as a reductant. The lower a reaction occurs on the diagram the more stable the product is, meaning that the metal reactant has a higher affinity for oxidation. With an increase in temperature, the ΔG of these oxide reactions also increases. This means that the oxide products are less stable at higher temperatures. If a plotted equation extends above zero, spontaneous thermal dissociation of this oxide into oxygen and metal is thermodynamically favoured in an isolated system (Rosenqvist, 2004).

The calculation of Gibbs free energy presumes constant temperature and pressure. Therefore, for the generation of an Ellingham diagram where temperature is used as the x-axis variable, the pressure is assumed to be constant. To see the effect of pressure on the ΔG it is necessary to consider enthalpy in more detail. Expanding the enthalpy function in Equation 2 gives Equation 3 where U is internal energy (J), V is volume (m^3), and P is pressure (Pa).

$$\Delta G = \Delta U + P \Delta V - T \Delta S \tag{3}$$

Ellingham Diagram
Modelled at 1atm absolute ambient pressure

Diagram axes: ΔG° (kJ) vs Temperature (°C)

Reactions labelled:
$2C + O_2 \Rightarrow 2CO$
$4K + O_2 \Rightarrow 2K_2O$
$4Na + O_2 \Rightarrow 2Na_2O$
$2CO + O_2 \Rightarrow 2CO_2$
$2H_2 + O_2 \Rightarrow 2H_2O$
$C + O_2 \Rightarrow CO_2$
$2Fe + O_2 \Rightarrow 2FeO$
$\frac{4}{3}Cr + O_2 \Rightarrow \frac{2}{3}Cr_2O_3$
$2Mn + O_2 \Rightarrow 2MnO$
$Si + O_2 \Rightarrow SiO_2$
$Ti + O_2 \Rightarrow TiO_2$
$\frac{4}{3}Al + O_2 \Rightarrow \frac{2}{3}Al_2O_3$
$2Mg + O_2 \Rightarrow 2MgO$
$2Ca + O_2 \Rightarrow 2CaO$

State Changes	Metal	Oxide
Melting Point	M	[M]
Boiling Point	B	[B]
Transition Point	T	[T]

FIG 1 – Ellingham diagram for the formation of various common lunar oxides at 1 atm pressure

Transitions:

T_1	Ca	FCC to BCC
T_2	Ti	HCP to BCC
$[T]_3$	SiO$_2$	α-Quartz to β-Quartz
$[T]_4$	SiO$_2$	β-Quartz to β-Tridymite
$[T]_5$	SiO$_2$	β-Tridymite to β-Cristobalite

Transitions:

T_6	Mn	CBCC to SC
T_7	Mn	SC to FCC
T_8	Mn	FCC to BCC
$[T]_9$	Na$_2$O	S1 to S2
$[T]_{10}$	Na$_2$O	S2 to S3
T_{11}	Fe	BCC to FCC

FCC = Face Centred Cubic
BCC = Body Centred Cubic
CBCC = Complex Body Centred Cubic
HCP = Hexagonal Close-Packed
SC = Simple Cubic

Modelling completed in the FactSage 7.2 thermochemical software package.

In theory, the magnitude of the constant pressure can be anything, however, in practice, all readily available Ellingham diagrams are calculated at 1 atm pressure. For terrestrial industry and practical metallurgy the 1 atm Ellingham diagram makes sense. However, for an investigation into the effects of high-vacuum on metallurgical processes, and especially in the context of space exploration and materials processing, the assumed constant pressure of 1 atm is completely arbitrary. The generation of basic Ellingham diagrams for some common oxide species at varying pressures allows for an easy way to visualise the effect of pressure on the stability of these oxide species. The oxides chosen in the current work are all common oxides found on the lunar surface (Papike, Simon and Laul, 1982; McKay *et al*, 1991). Some common reductants such as C, CO, and H_2 have also been included.

Low pressure Ellingham diagrams

In order to investigate the practical effects of pressure on oxide stability, a series of 'standard' Ellingham diagrams were created at four distinct pressures. The four chosen pressures represent the four rough tiers of vacuum, these tiers and their significance, are described in Table 1. The colloquial designation of the vacuum tiers varies significantly depending on source, each level is often associated with a range of pressures. The pressures chosen here to represent the different tiers are therefore rough generalisations.

TABLE 1

The pressures used for Ellingham diagram generation and their significance.

Colloquial designation	Pressure	Significance
No vacuum	1 atm	Normal operation on Earth's surface.
Low vacuum	10^{-5} atm	The pressure reasonably attainable in terrestrial industry with mechanical pumps.
High vacuum	10^{-10} atm	The pressure attainable in industry and labs using specialised pumping equipment.
Ultra-high vacuum	3×10^{-15} atm	The ambient pressure measured on the lunar surface at night; attainable in labs using very specialised pumping equipment.

Ellingham diagrams generated at 1 atm, 10^{-5} atm, 10^{-10} atm, and 3×10^{-15} atm are shown in Figures 1, 2, 3 and 4 respectively. The data for these diagrams was obtained using the reaction module in the FactSage 7.2 thermochemical modelling software. The databases used for the modelling were FactPS and FTOxid. All phase changes and transition points have been marked. Lines for the carbon and hydrogen reduction steps have been added for reference as per the standard Ellingham diagram. Further detail on the FactSage modelling package can be found elsewhere (Bale *et al*, 2002, 2009, 2016; CRCT-PC).

In the standard 1 atm Ellingham diagram, Figure 1, the majority of the oxides are found well below the C to CO_2 line with only Cr_2O_3, FeO, K_2O, and Na_2O being viable options for reduction with C. The diagram has a y-axis maximum of 0 with only Na and K able to be spontaneously thermally reduced in the 0 to 2000°C temperature range. The majority of the plotted oxides trend towards a positive ΔG^0 with extrapolated intersects well above 3000°C. This diagram differs from the common oxide Ellingham diagram only in that the oxides plotted represent those 10 major oxides found on the lunar surface omitting for example Fe_2O_3 which, whilst common on Earth, is not seen in high concentrations on the lunar surface (Papike, Simon and Laul, 1982; McKay *et al*, 1991).

Ellingham Diagram
Modelled at 1×10^{-5} atm absolute ambient pressure
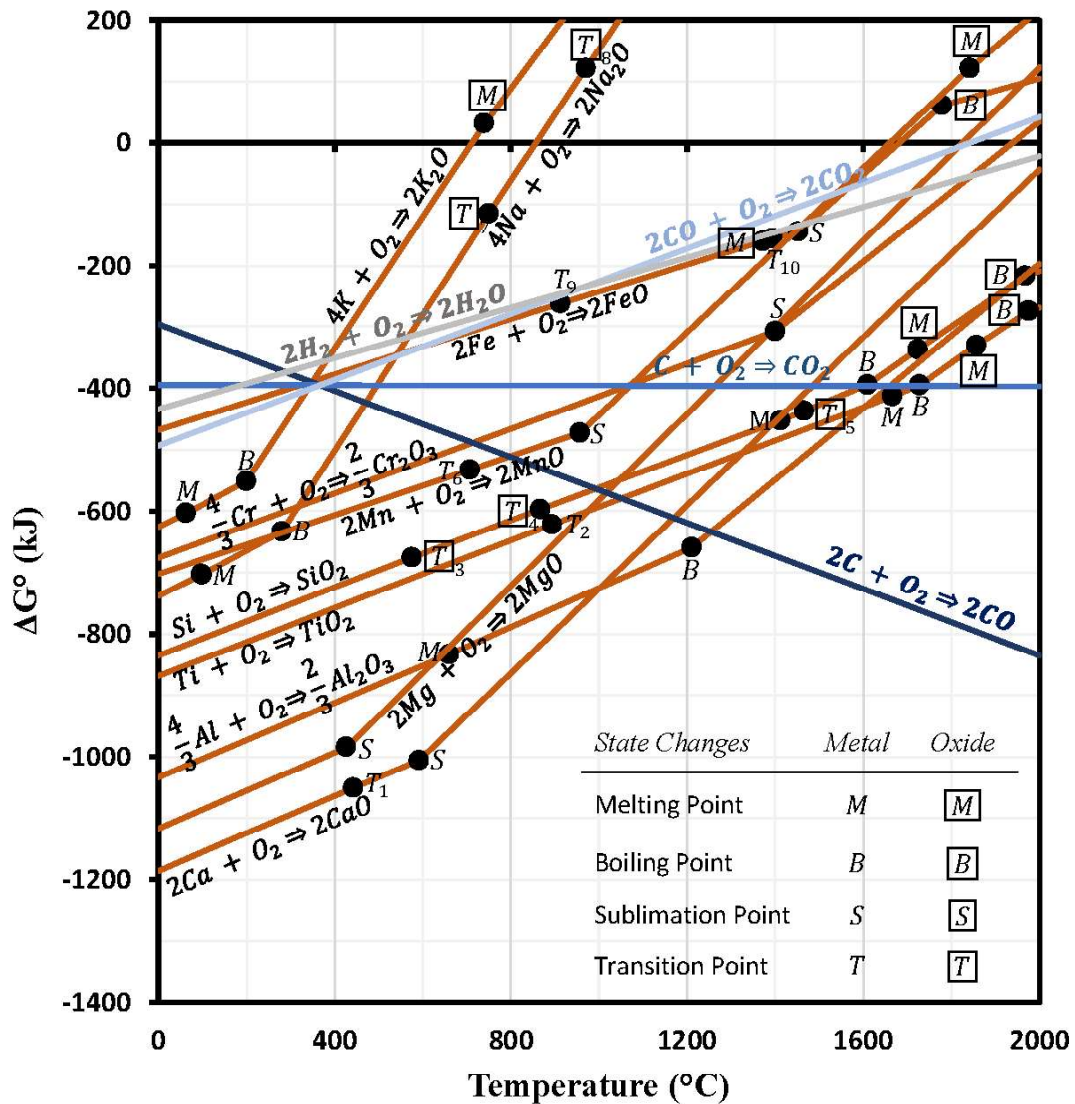
Transitions:

T_1	Ca	FCC to BCC
T_2	Ti	HCP to BCC
$\boxed{T}_3$	SiO$_2$	α-Quartz to β-Quartz
$\boxed{T}_4$	SiO$_2$	β-Quartz to β-Tridymite
$\boxed{T}_5$	SiO$_2$	β-Tridymite to β-Cristobalite

Transitions:

|		
T_6	Mn	CBCC to SC
$\boxed{T}_7$	Na$_2$O	S1 to S2
$\boxed{T}_8$	Na$_2$O	S2 to S3
T_9	Fe	BCC to FCC
T_{10}	Fe	FCC to BCC

FCC = Face Centred Cubic
BCC = Body Centred Cubic
CBCC = Complex Body Centred Cubic
HCP = Hexagonal Close-Packed
SC = Simple Cubic

Modelling completed in the FactSage 7.2 thermochemical software package.

FIG 2 – Ellingham diagram for the formation of various common lunar oxides at 10^{-5} atm pressure.

Ellingham Diagram
Modelled at 1×10^{-10} atm absolute ambient pressure
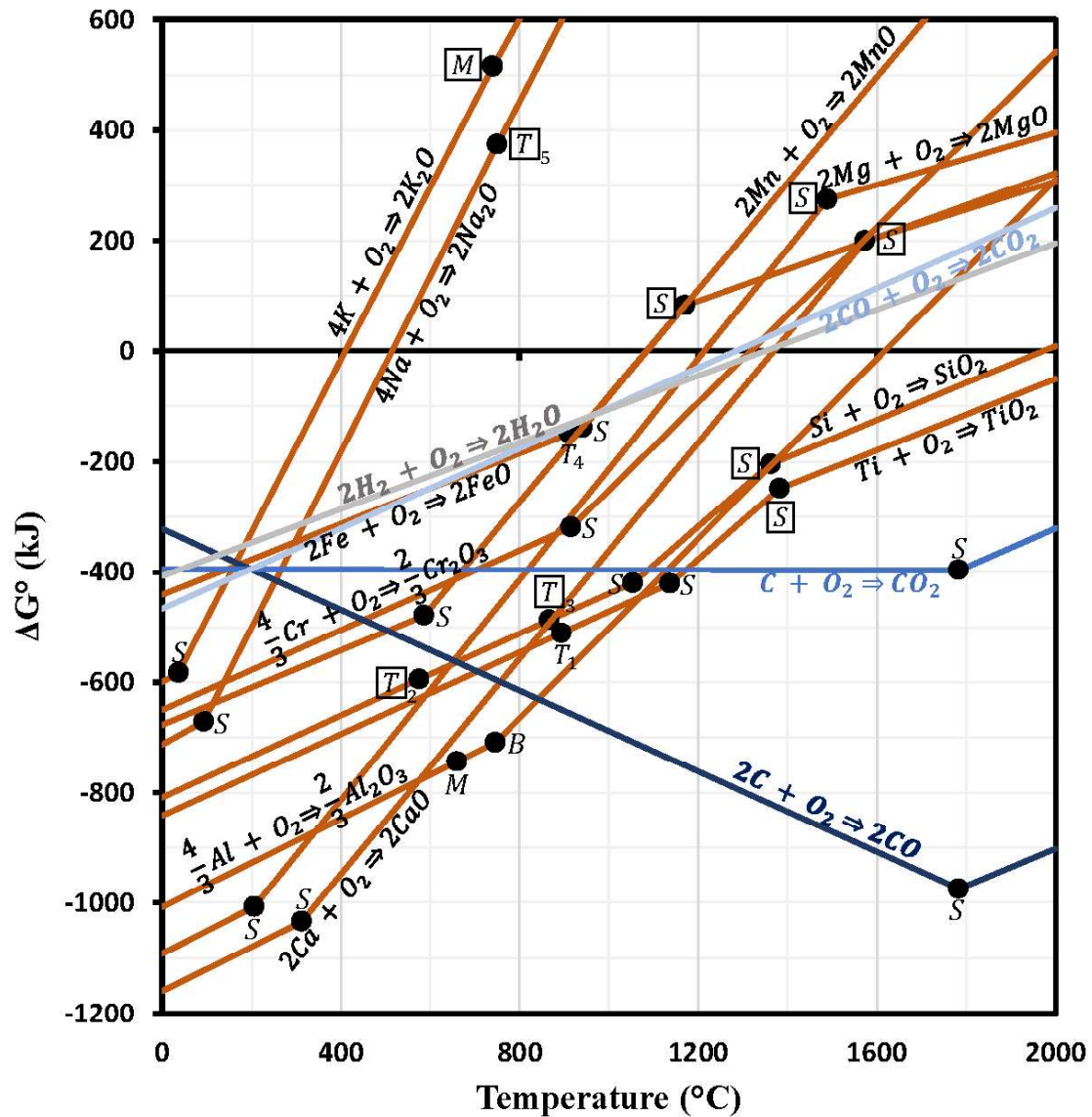
Transitions:		
T_1	Ti	HCP to BCC
$\boxed{T}_2$	SiO$_2$	α-Quartz to β-Quartz
$\boxed{T}_3$	SiO$_2$	β-Quartz to β-Tridymite
T_4	Fe	BCC to FCC
$\boxed{T}_5$	Na$_2$O	S1 to S2

State Changes	Metal	Oxide
Melting Point	M	$\boxed{M}$
Boiling Point	B	$\boxed{B}$
Sublimation Point	S	$\boxed{S}$
Transition Point	T	$\boxed{T}$

Modelling completed in the FactSage 7.2 thermochemical software package.

FIG 3 – Ellingham diagram for the formation of various common lunar oxides at 10^{-10} atm pressure.

Ellingham Diagram
Modelled at 3×10^{-15} atm absolute ambient pressure
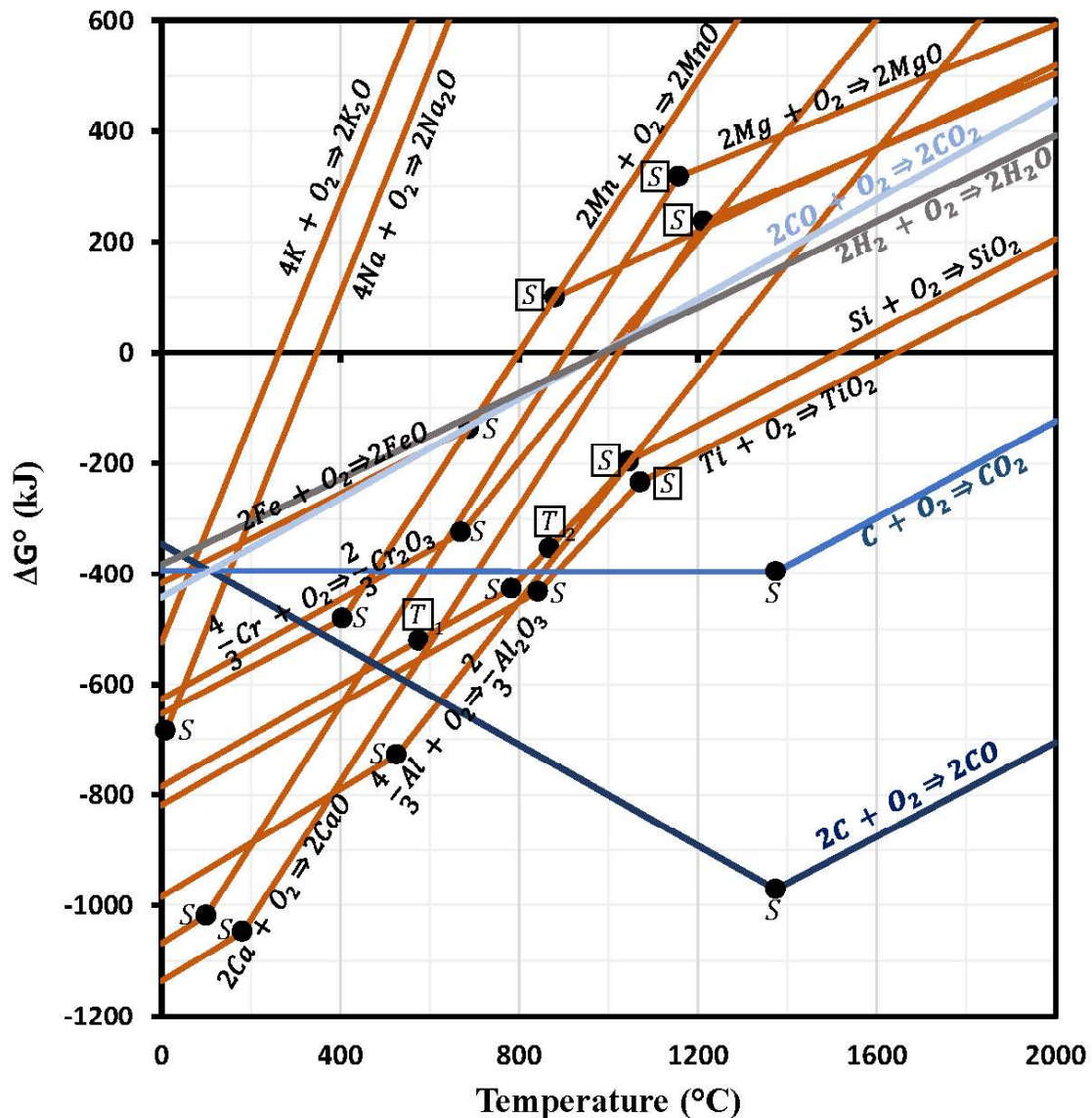
Transitions:		
T_1	SiO_2	α-Quartz to β-Quartz
T_2	SiO_2	β-Quartz to β-Tridymite

State Changes	Metal	Oxide
Melting Point	M	M
Boiling Point	B	B
Sublimation Point	S	S
Transition Point	T	T

Modelling completed in the FactSage 7.2 thermochemical software package.

FIG 4 – Ellingham diagram for the formation of various common lunar oxides at 3×10^{-15} atm pressure.

Moving to a total pressure of 10^{-5} atm, Figure 2 shows some small but significant changes when compared to the standard 1 atm Ellingham diagram. The thermal dissociation of Cr, Mg, Fe, Mn, along with Na and K, is now thermodynamically favoured below 2000°C. Notice also that due to the change in ΔS in the Mg reaction line by the sublimation of Mg at ~430°C, the Mg and Si reaction

lines now cross at ~1050°C. This means that at 10^{-5} atm, and above 1050°C, MgO will spontaneously be reduced by Si metal, which, as discussed above, is known as the Pidgeon process. The reason we point this out is that when looking at a normal Ellingham diagram, reconciliation of the data provided therein with the industrially used Pidgeon process can be somewhat confusing, this is one of the benefits of generating entire Ellingham diagrams at differing pressures. Also of note within Figure 2, all plotted oxides are able to be reduced by solid carbon below 2000°C. It is important to observe at this point that the diagrams depicted here are intended as a visual representation of the effect of vacuum on oxide stability. The Ellingham diagram is limited in the sense that it cannot be relied upon to accurately predict a reaction sequence without the inclusion of all relevant reactions. The oxide version found in Figures 1–4 ignores, for example, the formation of carbides which may result in an even lower Gibbs free energy for the system. Ellingham diagrams of sulfides, chlorides, fluorides, carbides, carbonates, silicates, aluminates etc at 1 atm pressure can be found elsewhere (Rosenqvist, 2004), although diagrams at reduced pressures have not been generated to date in the manner presented here.

Figure 3, generated at 10^{-10} atm, represents high-vacuum conditions. These conditions are theoretically attainable on Earth using complicated pumping systems but are readily available in space. Some interesting trends when compared to the higher-pressure diagrams can be seen. All plotted oxides barring TiO_2, CO_2, and CO spontaneously thermally dissociate below 2000°C. A number of the metals and oxides now undergo sublimation rather than melting and boiling, and significantly fewer transitions (described below the diagram) take place. Carbothermal reduction of most of the oxides is now predicted to be feasible below 800°C. The y-axis maximum has been moved to 600°C in this figure to show more information.

The final diagram, Figure 4, at 3×10^{-15} atm pressure, moves into the realm of the theoretically pristine lunar environment. Of all the diagrams presented in the current work this one is considered the most theoretical as the operation of a reactor under these conditions, considering the inherent gas generation, would be rendered kinetically impossible. However, in the interest of presenting extreme, but theoretically attainable conditions, it has been included. At this pressure, carbon is predicted to sublimate before 1400°C and all plotted oxides apart from CO_2 and CO are predicted to be unstable above 1650°C with Cr_2O_3, MnO, MgO, FeO, H_2O, CO_2, K_2O, and Na_2O all being unstable above 1000°C. Only SiO_2 is predicted to undergo any phase transitions (from α-quartz to β-quartz and then to β-tridymite) at this temperature. Note the lack of liquid phases as direct sublimation is favoured for all products and reactants at this pressure.

SPACE AS A PLATFORM FOR HIGH VACUUM METALLURGY

While pumping equipment and the increased process complexity of operating vacuum processes on Earth are limiting, the field of astrometallurgy does not suffer from these restrictions. High (10^{-10} atm) and even ultra-high ($<<10^{-10}$ atm) vacuum conditions are readily available in space just as 1 atm conditions are readily available on Earth. Similarly, whereas on Earth energy is relatively cheap, access to electrical energy on the Moon will be significantly more limited, therefore the design of astrometallurgical processes will favour low energy consumption more so than in designs for terrestrial application.

With access to what could be considered 'industrial quantities' of high vacuum, the feasibility of using vacuum metallurgy is no longer restricted by acquisition and instead more technical concerns come into play. Issues such as reaction kinetics at low temperatures, mass transport within the reactants, rapid removal of product gases, evaporation and sublimation rates, and efficient condensing apparatus' that do not lose product to the natural vacuum, will play larger roles. Historically, little research has been done in these areas as the access to vacuum has been a significant enough limiting factor that the rest are not considered important. However, with an expansion of operations into space, and more importantly the easier access to such vacuum conditions for research purposes, a deeper understanding of these specific limiting mechanisms within vacuum metallurgical operations will become possible. While this targeted research will almost certainly be aimed at the development of astrometallurgical processes, the knowledge gained will be extremely applicable to terrestrial vacuum metallurgy technologies and may increase the viability of using vacuum in a wider variety of areas on Earth.

The exciting prospect of access to essentially infinite ultra-high vacuum conditions aside, when it comes to industrial resource processing in space, the 'contamination' of the natural vacuum should be considered. Whilst any short-term artificial 'atmosphere' created by the venting of gases in space will eventually dissipate, the continual discharge of gaseous species as part of an industrial process could lead to a semi-permanent 'contamination', or increase in pressure, of the ambient vacuum. This should ideally be avoided, both in terms of maintaining the clean environment of space, but also to avoid the deposition of miscellaneous materials on the outside of equipment and sensors in the local area. Large pressure spikes on the Moon as a result of human activity have been reported; with such low natural pressures on the Moon it is estimated that the act of launching the return stage of the Apollo missions *doubled* the total mass of the *entire* lunar atmosphere (Vondrak, 1992). This added gas naturally dissipated over time, however, herein lies the source of the reasoning mentioned previously of the active lunar pressure during prolonged human or robotic presence on the Moon. A constant pressure of 3×10^{-15} atm is not expected during industrial activities and human presence on the Moon, the ambient pressure will have to be monitored and balanced with activities (both industrial and other) resulting in gas discharge. The careful control of ambient pressures will be important for prolonged industrial activity on the lunar surface both in terms of detrimental process inhibiting effects and societal license to operate.

CONCLUSIONS

Vacuum metallurgy is understood to be beneficial in some circumstances on Earth but is severely limited by pumping technology. Some industrial processes do operate at low pressures using mechanical vacuum pumps, such as the Pidgeon process for magnesium production, however high vacuum conditions (10^{-10} atm) have to date not been used in large scale metal reduction processes on Earth.

Despite the issues inherent in the application of high vacuum conditions to terrestrial resource processing, an understanding of the potential benefits of these conditions is still relevant. The current work has aimed to highlight the significant thermodynamic effects of vacuum conditions of the stability of oxides. Four Ellingham diagrams modelled using the FactSage thermochemical software at pressures of 1, 10^{-5}, 10^{-10}, and 3×10^{-15} atm have been presented and described here. Analysis of these diagrams shows that oxides under vacuum conditions require significantly less energy for reduction to take place. It is also noted that the use of Ellingham diagrams to display the effect of vacuum on a system can remove some confusion when analysing processes such as the Pidgeon process which, when analysed using a standard Ellingham diagram, generated at 1 atm pressure, is not thermodynamically viable at the temperatures used in industry.

Space provides us with an excuse and a platform to further explore vacuum metallurgy as an area of research. The potential benefits of high-vacuum conditions on industrial processing operations are known but have been hindered historically by our lack of access to these vacuum conditions. The application of high vacuum metallurgy in astrometallurgical processes, ie resource processing in space, has significant merit. It will lead both to the development of metal extraction techniques that simply aren't feasible on Earth, but also to a deeper understanding of the vacuum metallurgical applications that can be used on Earth.

In 1951, Kroll stated that 'In the course of time it [vacuum metallurgy] will firmly entrench itself in the front line of a steadily advancing metallurgy' (Kroll, 1951). Over 70 years later this statement is more relevant than ever.

ACKNOWLEDGEMENTS

REFERENCES

Bale, C W, Bélisle, E, Chartrand, P, Decterov, S, Eriksson, G, Gheribi, A, Hack, K, Jung, I-H, Kang, Y-B and Melançon, J, 2016. Reprint of: FactSage thermochemical software and databases, 2010–2016. *Calphad,* 55**,** 1–19.

Bale, C W, Chartrand, P, Degterov, S, Eriksson, G, Hack, K, Mahfoud, R B, Melançon, J, Pelton, A and Petersen, S, 2002. FactSage thermochemical software and databases. *Calphad,* 26**,** 189–228.

Bale, C, Bélisle, E, Chartrand, P, Decterov, S, Eriksson, G, Hack, K, Jung, I-H, Kang, Y-B, Melançon, J and Pelton, A, 2009. FactSage thermochemical software and databases—recent developments. *Calphad,* 33, 295–311.

Balomenos, E, Panias, D and Paspaliaris, İ, 2012. Exergy Analysis of Metal Oxide Carbothemic Reduction under Vacuum–Sustainability prospects. *International Journal of Thermodynamics,* 15, 141–148.

Browne, J R, 1971. A review of the fundamentals of vacuum metallurgy. *Vacuum,* 21, 13–16.

CRCT-PC. *FactSage Database Documentation* [Online]. Available: http://www.crct.polymtl.ca/fact/documentation/ [Accessed 15/09/2019].

Ellingham, H J T, 1944. Reducibility of oxides and sulfides in metallurgical processes. *J Soc Chem Ind,* 63, 125–133.

Halmann, M, Frei, A and Steinfeld, A, 2008. Magnesium production by the pidgeon process involving dolomite calcination and MgO silicothermic reduction: thermodynamic and environmental analyses. *Industrial and Engineering Chemistry Research,* 47, 2146–2154.

Halmann, M, Frei, A and Steinfeld, A, 2011. Vacuum Carbothermic Reduction of Al_2O_3, BeO, MgO-CaO, TiO_2, ZrO_2, HfO_2 + ZrO_2, SiO_2, SiO_2 + Fe_2O_3, and GeO_2 to the Metals. A Thermodynamic Study. *Mineral Processing and Extractive Metallurgy Review,* 32, 247–266.

Kroll, W, 1951. Vacuum metallurgy: its characteristics and its scope. *Vacuum,* 1, 163–184.

Mckay, D S, Heiken, G, Basu, A, Blanford, G, Simon, S, Reedy, R, French, B M and Papike, J, 1991. The lunar regolith. *Lunar sourcebook,* 285–356.

O'Hanlon, J F, 2005. *A user's guide to vacuum technology*, John Wiley and Sons.

Papike, J, Simon, S B and Laul, J, 1982. The lunar regolith: Chemistry, mineralogy, and petrology. *Reviews of Geophysics,* 20, 761–826.

Pidgeon, L and Alexander, W, 1944. Thermal production of magnesium-pilot plant studies on the retort ferrosilicon process. *Transactions AIME,* 159, 315–352.

Rankin, W J, 2011. *Minerals, Metals and Sustainability: Meeting Future Material Needs*, CSIRO publishing.

Rosenqvist, T, 2004. *Principles of Extractive Metallurgy*, Trondheim, Norway: Tapir Academic Press.

Roth, A, 1990. *Vacuum technology,* Amsterdam/New York.

Vondrak, R R, 1992. Lunar base activities and the lunar environment. NASA Conference Publication. NASA, 337–337.

Wada, Y, Fujii, S, Suzuki, E, Maitani, M M, Tsubaki, S, Chonan, S, Fukui, M and Inazu, N, 2017. Smelting magnesium metal using a microwave Pidgeon method. *Scientific Reports,* 7, 1–7.

Zang, J C and Ding, W, 2016. The Pidgeon process in China and its future. *Essential Readings in Magnesium Technology.* Springer.